ELSEVIER

Surface Science 515 (2002) 431–440

SURFACE SCIENCE

www.elsevier.com/locate/susc

Hydrothermal growth of $BaTiO_3$ on TiO_2 single crystals

Judit G. Lisoni [a,*,1], C.H. Lei [b], T. Hoffmann [a,1], V.M. Fuenzalida [a]

[a] *Universidad de Chile, Departamento de Física, Avda. Blanco Encalada 2008, Casilla 487-3, Santiago 6611226, Chile*
[b] *EMAT, RUCA, University Antwerp, Groenenborgerlaan 171, B-2020, Antwerp, Belgium*

Received 7 November 2000; accepted for publication 29 May 2002

Abstract

The hydrothermal growth of polycrystalline $BaTiO_3$ deposits on the surface of TiO_2 rutile single crystals has been studied with respect to the following parameters: (a) small quantities of Sr (1.0 and 0.04 at.%) in the $Ba(OH)_2$ aqueous solution and (b) crystallographic surface of TiO_2. For this purpose, the substrates were immersed in hydrothermal baths at temperatures between 100 and 200 °C for 4 h. It was found that the deposits grown with the high purity $Ba(OH)_2$ reagent (Sr $\sim$ 0.04 at.%) exhibited grains with a pronounced crystal habit of octahedral shape with well-defined {1 1 1} faces. The grains grew at temperatures as low as 100 °C. The strontium rich $Ba(OH)_2$ solution (Sr $\sim$ 1.0 at.%) led to grains of spherical shapes, which appeared only at temperatures of 150 °C and above. The use of single crystal substrates with different orientations strongly influences the growth of the $BaTiO_3$ layer: the same treatment to deposit $BaTiO_3$ on the (0 0 1) TiO_2 face did not produce $BaTiO_3$ on the (1 1 0) surfaces. This result can be interpreted in term of the stability of the single crystal surfaces and the related dissolution of TiO_2. The samples were characterized by means of XRD, RBS, EDX, XPS, SEM (secondary and backscattered electrons), WDS, TEM and AFM.

Keywords: Models of surface kinetics; Scanning electron microscopy (SEM); Transmission high-energy electron diffraction; Growth; Nucleation; Titanium oxide; Low index single crystal surfaces; Polycrystalline thin films

1. Introduction

Since 1989 the hydrothermal method has been used for the low-temperature fabrication of polycrystalline $BaTiO_3$ thin films on different kinds of substrates, e.g.: Ti foil [1], glass\Ti [2], Si\Pt\Ti [3] and TiO_2(0 0 1) [4]. The technique consists in introducing the substrate in an alkaline aqueous solution of $Ba(OH)_2$ at temperatures between 55 °C [5] and 600 °C [6] for a few hours. This procedure leads to polycrystalline $BaTiO_3$ film, which covers the exposed Ti surface, which exhibits good adherence to the substrate. It is known that the thickness, microstructure and crystallinity of these films depend on the processing parameters such as temperature, barium concentration, pH, reaction time, and on the potential and current density if the process is electrochemically activated.

The microstructure of the films grown hydrothermally on metallic substrates is a polycrystalline aggregate with a cauliflower-like structure [1]. Grain size has been reported to decrease with

* Corresponding author. Fax: +32-16-28-12-14.
E-mail address: lisonij@imec.be (J.G. Lisoni).
[1] Present address: IMEC vzw, Silicon Process Technology Division, Kapeldreef 75, B-3001, Leuven, Belgium.

0039-6028/02/$ - see front matter
PII: S0039-6028(02)01959-3

increasing $Ba(OH)_2$ concentration and with increasing temperature [7], exhibiting a more regular grain size with increasing strontium content when $Ba(OH)_2 + Sr(OH)_2$ solutions of various relative concentrations are used [8].

Several workers have investigated the growth kinetics of $BaTiO_3$ under hydrothermal conditions either as powders [9,10] or thin films [1,5–8,11–15]. In the latter case and because of its potential applications, the investigations have been mainly focused on the electrochemical activation. Ishizawa et al. reported about a precursor anatase layer between the titanium metal foil and the electrochemically grown $BaTiO_3$ film [11]. Bendale et al. proposed a film growth mechanism in which the first step was the formation of a titanium oxide layer [12]. Therefore, the initial growth of the films is controlled by charge transfer, correlated to the oxidation of titanium and, later on, by mass transfer as it was demonstrated by Vargas et al. [13]. The spontaneous initial nucleation linked to pure hydrothermal $BaTiO_3$ formation can be inhibited by cathodically protecting the titanium electrode, leading to no film growth, and the application of initial nucleation potential affected the grain size of a subsequent deposit once the cathodic protection was removed [14]. A recent review proposes the formation of an anodic TiO_x film, which dissolves in water as titanate ions $[Ti(IV)O_x]^{4-2x}$ [15]. Thereafter, the chemical reaction between the barium and the titanate ions leads to the nucleation of $BaTiO_3$ crystallites on the substrate surface, as depicted in the scheme of Fig. 8 of Ref. [15].

Although there is less information on the kinetics of pure hydrothermal growth of thin films, it is generally accepted that the growth proceeds through dissolution–precipitation, and that the formation of a precursor oxide is a necessary step. Therefore, the study of the growth of $BaTiO_3$ on titanium oxide surfaces is mandatory in order to understand how the hydrothermal films grow on titanium. The use of oxide substrates has been reported either by starting with preoxidized titanium [16] or by using single crystal substrates [4], both reporting tetragonal $BaTiO_3$. Films grown on TiO_2 previously deposited on silicon by ion-beam assisted deposition exhibited (1 1 1) orientation [17]. None of these works addressed the growth mechanisms and kinetics.

In the present paper the use of single crystal titanium oxides as substrates provides a model system for analyzing some remaining variables involved in the purely hydrothermal $BaTiO_3$ film growth. The effect of the strontium at very low concentration and the influence of the titanium oxide crystal surface exposed to the aqueous solution are parameters which have not been discussed in the current literature, although the influence of high strontium concentrations has been reported [8,18]. We will show that the microstructure is strongly influenced by small amounts of strontium and that the growth kinetics strongly depends on the face of the single crystal exposed to the solution.

2. Experimental procedure

The substrates were single crystals of TiO_2, rutile, $10 \times 10 \times 0.5$ mm^3 in size, polished on both sides, (0 0 1) and (1 1 0) oriented (Crystal and Coating Technology, and Marketech., Inc.). Their root-mean-square (r.m.s.) surface roughness measured by AFM was about 0.7 nm, for both orientations.

The working solutions were prepared dissolving two different qualities of $Ba(OH)_2$ in 0.2 l of boiled deionized water in order to prevent the formation of $BaCO_3$. The reagent with maximum 1.0 at.% Sr impurity will be referred to as the "strontium rich" whereas the one with a maximum of 0.04 at.% Sr as the "high purity" reagent. The substrates were submerged during 4.0 h in a 0.5 M $[Ba^{+2}]$ solution in a Teflon vessel inside an autoclave. The treatment temperatures were 100, 150, and 200 °C. Afterward, the samples were shortly cleaned in an ultrasonic bath in order to eliminate the $BaCO_3$ surface residues. All the sample preparation experiments were performed twice.

The crystallographic phases were identified with X-ray diffraction (XRD, Siemens D5000 model) by using a non-monochromatic Cu Kα radiation (0.15418 nm). Typical scan rates were 0.02° per 10 s. The $BaTiO_3$ unit cell parameters were calculated by using the 0 0 4 TiO_2 rutile reflex as an

internal standard and the FINAX refinement parameter software [19]. Transmission electron microscopy (TEM, JEOL 2000EX) was performed at 200 kV. Conventional routines, i.e., cutting, grinding, dimpling, polishing and final ion milling were applied to prepare cross-sectional samples for structural study.

The sample composition was investigated by means of X-ray photoelectron spectroscopy (XPS, Physical Electronics 1257 system, Al Kα non-monochromatic radiation), backscattered electrons of the SEM, energy and wavelength dispersive spectroscopy (EDX and WDS, respectively) and Rutherford backscattering (RBS, TANDEM system, NEC model 5SDH) with α-particles of 2.0 MeV and a beam spot of approximately 2 mm in diameter.

Sample topography was characterized by means of scanning electron microscopy (SEM, JEOL models JSM-25-S2 and 6400, and Philips SFEG XL30) and atomic force microscopy in the tapping mode (AFM, Digital Instruments, MMAFM^{TM}).

3. Results

Table 1 summarizes the most important results obtained for the different TiO_2 single crystal orientations, Sr-content in the $Ba(OH)_2$ solution and temperatures used for the $BaTiO_3$ deposition.

3.1. $BaTiO_3$ on $TiO_2(0\,0\,1)$ prepared with different qualities of barium hydroxide reagent

3.1.1. Crystallographic characterization

Phase identification of the samples treated with the strontium-rich reagent in the case of TiO_2-(0 0 1) single crystals has been published elsewhere [4]. In brief, samples were reported to be cubic if grown at 150 °C and tetragonal if grown at 200 °C.

The purest hydroxide reagent produced only cubic $BaTiO_3$ deposits even at 100 °C (Fig. 1a). However, at this temperature the 1 1 0 $BaTiO_3$ reflex was too weak to calculate the unit cell parameter. Samples prepared at 150 and 200 °C displayed an unit cell value of 0.4035(5) nm, which did not exhibit any dependence on the preparation temperature. This value agrees with the tabulated one for cubic $BaTiO_3$ ($a = 0.4031$ nm) within the experimental error.

On the other hand, XRD recordings of the samples prepared with the strontium rich $Ba(OH)_2$ (Fig. 1b) at 100 °C did not show any reflections from $BaTiO_3$. At 150 °C the samples were cubic with a measured lattice parameter of 0.3990(5) nm,

Table 1
Summary of the most important results of the $BaTiO_3$ hydrothermal growth onto different TiO_2 single crystal surfaces

	TiO_2(0 0 1)						TiO_2(1 1 0)		
	Sr ~ 1.0 at.%			Sr ~ 0.04 at.%			Sr ~ 0.04 at.%		
	100 °C	150 °C	200 °C	100 °C	150 °C	200 °C	100 °C	150 °C	200 °C
$BaTiO_3$ crystallinity	No	Cubic	Cubic and tetragonal: double layer	Cubic	Cubic	Cubic	No $BaTiO_3$ was detected		
Lattice parameter (nm)	–	0.3990(5)	0.3994(4) 0.4040(6)	0.4035(5)	0.4035(5)	0.4035(5)	–	–	–
Sr:Ba content (at.%)	–	~10.0	~10.0	<1.0	<1.0	<1.0	–		
Morphology	Smooth as the initial single crystal surface	Isolated hemispherical grains. Barium localized in the grains	Continuous $BaTiO_3$ film: coalescence of the grains observed at 150 °C	Isolated grains (diameters <100 nm)	Isolated octahedral grains. Barium localized in the grains	Continuous $BaTiO_3$ film: dendrites	A few octahedral grains observed along the surface defects (polished lines)		

The crystallographic results were obtained by XRD and TEM, Sr:Ba ratio by RBS and EDX, morphology by SEM and AFM and microcomposition by WDS and backscattered electrons.

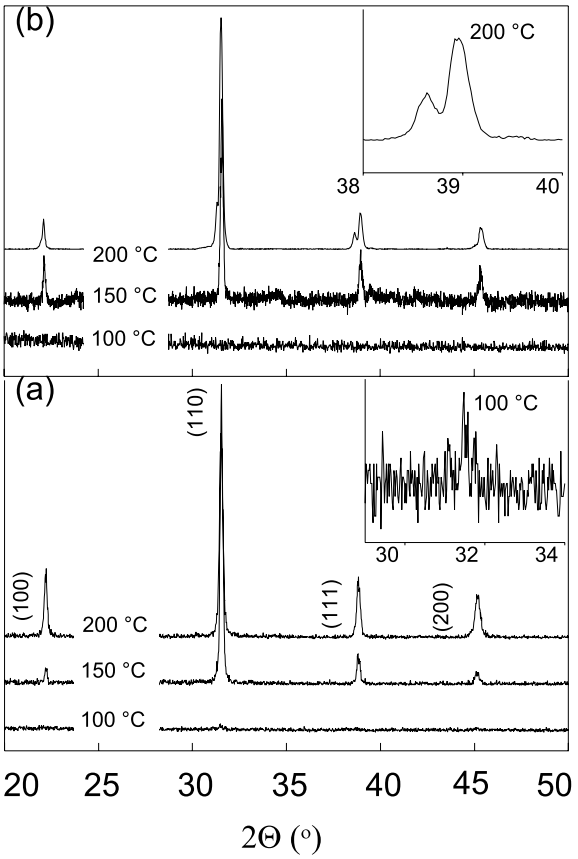

Fig. 1. XRD diffractograms of $BaTiO_3$ samples grown on TiO_2 (0 0 1) at the indicated temperatures with (a) high purity and (b) strontium rich $Ba(OH)_2$.

~1% smaller than that reported for cubic $BaTiO_3$ ($a = 0.4031$ nm). [2] The samples prepared at 200 °C exhibited additional reflections of tetragonal $BaTiO_3$ with parameters of 0.3994(4) and 0.4040(6) nm. A thorough interpretation of this result was obtained by TEM. A transversal view of the sample is depicted in Fig. 2. The film consisted of two layers formed by (a) fine and (b) coarse grains. The former, directly on top of the TiO_2 substrate, was between 50 and 800 nm thick. It displayed a columnar structure with an average grain size of approximately 50 nm. Only diffraction rings were obtained from these regions, indexed according to cubic $BaTiO_3$ (Fig. 3a). The TiO_2–$BaTiO_3$ interface was sharp showing no interdiffusion layer.

[2] Powder diffraction file (PDF of the Joint Committee for Powder Diffraction Standards (JCPDS)) no. 31-174 for cubic ($a = 0.4031$ nm) and no. 5-626 for tetragonal $BaTiO_3$ ($a = 0.3994$ nm, $c = 0.4038$ nm), respectively.

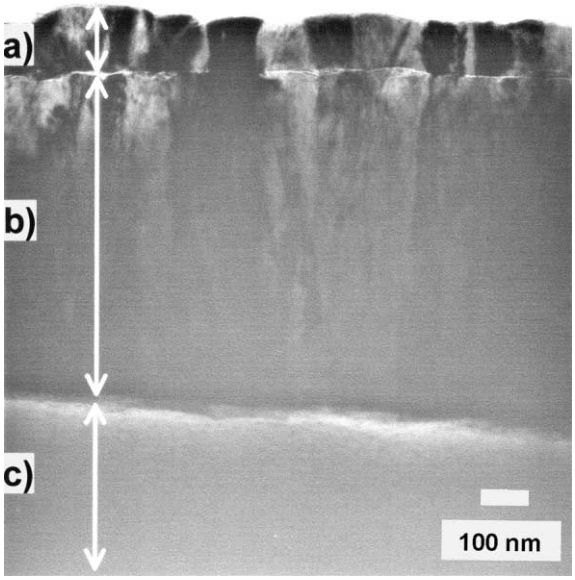

Fig. 2. TEM cross-sectional image of a TiO_2(0 0 1) sample treated 4 h at 200 °C with the Sr rich reagent: (a) coarse $BaTiO_3$ grains, (b) fine $BaTiO_3$ grains and (c) TiO_2(0 0 1) substrate.

The coarse grain layer also showed a wide range of thicknesses ranging from 50 to 200 nm. Electron diffraction patterns (EDP) of isolated grains along the [1 1 1] axis zone showed that two of the three (0 2 2) distances are not equivalent (Fig. 3b). The same observation holds true for the (0 1 0) and (0 0 1) distances along the [0 1 0] axis zone. Consequently, this measurement assigns the tetragonal structure to these grains. It is worth to mention that this kind of coarse grains was never observed on samples treated with the high purity reagent.

3.1.2. Strontium content

EDX spectra displayed the strontium signals only in samples fabricated with the Sr-rich reagent. Considering the detection limit of this technique it is possible to assure that the Sr content in samples prepared with the purest Ba-hydroxide is less than 1.0 at.%. Since the characteristic emission lines for titanium and barium are too close ($Ti\,K_\alpha = 4.51$ KeV, $K_\beta = 4.93$ keV; $Ba\,L_\alpha = 4.47$ keV) it

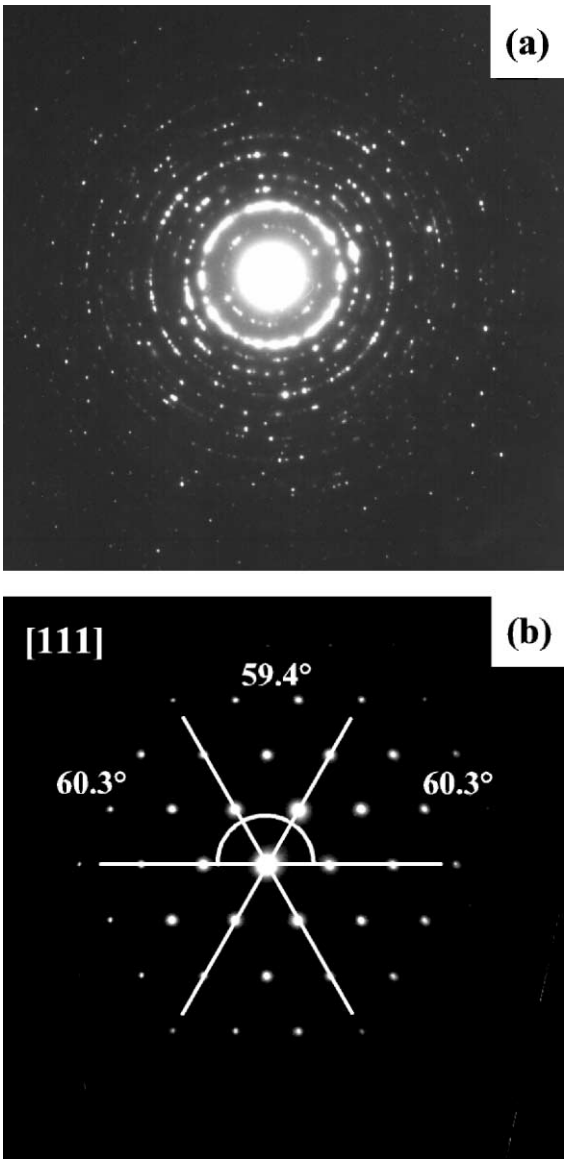

Fig. 3. EDP of the fine and coarse grain layers of Fig. 2. They correspond to (a) cubic and (b) tetragonal $BaTiO_3$, respectively. EDP in (b) was taken along the [1 1 1] axis zone.

was not possible to use EDX to quantify the Sr:Ba ratio.

Similar observations concerning the strontium content were obtained by RBS. In effect, strontium was only detected in samples treated with the strontium rich hydroxide (Fig. 4). The calculated value for the atomic ratio between strontium and

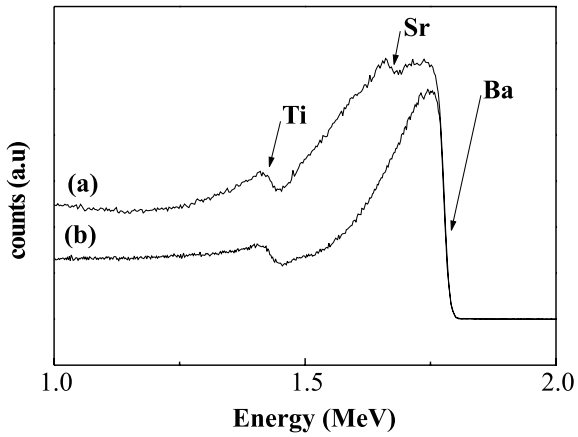

Fig. 4. RBS spectra of the TiO_2(0 0 1) samples treated at 200 °C during 4 h in (a) Sr rich and (b) high purity $Ba(OH)_2$.

barium (Sr:Ba) was approximately 0.1, for samples grown both at 150 and 200 °C. This is at least one order of magnitude larger than the corresponding proportion of the strontium rich hydroxide powder composition (1.0 at.%). This result suggests a major incorporation of strontium into the $BaTiO_3$ deposits, at least at the film surface region and down to a depth of 200 nm. Deposits obtained with the high purity $Ba(OH)_2$ did not show any signal attributable to strontium. In order to obtain a rough estimation for the upper limit of the strontium-content detection, an RBS simulation was performed. We supposed a homogeneous (Ba,Sr)TiO_3 layer of 200 nm in thickness on a TiO_2 substrate. If an atomic proportion of Sr:Ba $\sim$ 1:100 ($\sim 10^{14}$ Sr-atoms/cm^2) is assumed, the simulated strontium signal is buried under the barium signal. Therefore, if the strontium content in our samples is of the order of 1.0 at.% or lower, RBS will not detect it.

3.1.3. Microstructure and local composition

A comparison of the sample morphologies is presented in the set of SEM micrographs of Fig. 5. As shown in the micrographs the differences attributable to the different quality of the two hydroxides were the following:

(1) TiO_2(0 0 1) single crystals treated at 100 °C with the strontium-rich hydroxide displayed a surface quite similar to that observed in the

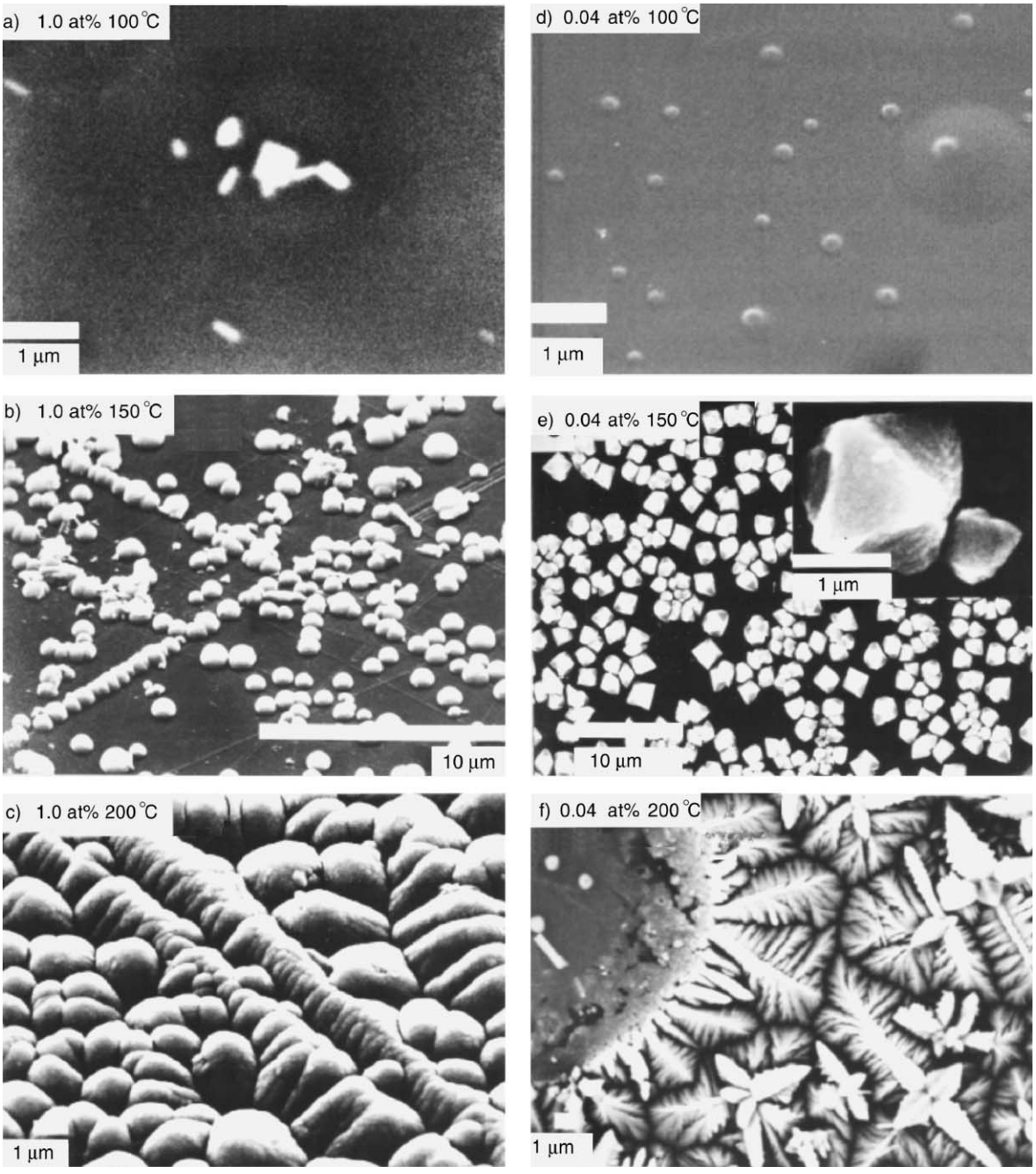

Fig. 5. SEM micrographs of $TiO_2(0\,0\,1)$ samples treated 4 h at the indicated temperatures and quality of the $Ba(OH)_2$ reagent.

single crystal without any treatment (Fig. 5a). A treatment with the high purity reagent at the same temperature leads to a rougher surface (Fig. 5d). The high purity reagent produced observable grains of $BaTiO_3$ at temperatures as low as 100 °C.

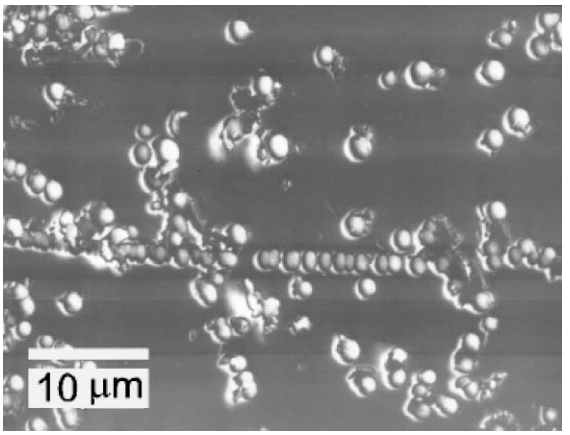

Fig. 6. Backscattered image of a $TiO_2(0\,0\,1)$ sample treated 4 h at 150 °C with the Sr rich reagent.

(2) The strontium rich hydroxide produced visible deposits only at temperatures of 150 °C and higher (Fig. 5b).
(3) The strontium rich reagent led to hemispherical shaped $BaTiO_3$ grains (Fig. 5b), whose coalescence is observed at 200 °C (Fig. 5c).
(4) The high purity hydroxide promotes the formation of grains with octahedral form (Fig. 5e) and with well-defined {1 1 1} faces (inset Fig. 5e). It suggests that these grains are single crystal domains of cubic $BaTiO_3$.
(5) At 200 °C the high purity hydroxide led to the formation of dendrites (Fig. 5f).
(6) SEM backscattered electron micrographs exhibited bright zones at the grains, associated to heavy atoms, and dark zones otherwise (Fig. 6). This information was confirmed by WDS, which correlated the location of barium with the position of the grains (Fig. 7). The figure shows large barium content inside a grain, which reduces to less than 15% on the flat surface away from the grains, estimated from the height of the barium peak.

3.2. $BaTiO_3$ on $TiO_2(1\,1\,0)$ made with the high purity barium hydroxide reagent

The results of this section correspond to samples prepared with the high purity reagent.

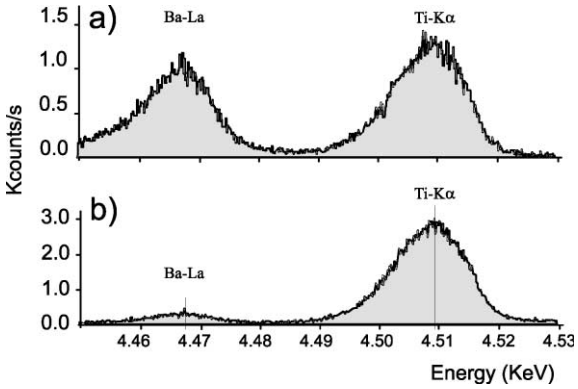

Fig. 7. WDS spectrum of a $TiO_2(0\,0\,1)$ sample treated 4 h at 150 °C with the high purity reagent, (a) inside and (b) outside of a grain.

3.2.1. Crystallographic characterization

In the whole range of temperatures investigated the samples grown onto $TiO_2(1\,1\,0)$ displayed only the reflections from the substrate and $BaCO_3$. The latter was removed after a short cleaning with an ultrasonic bath, suggesting that it is a surface contaminant not adhered to the substrate.

3.2.2. Microstructure

SEM micrographs revealed a surface free of islands in the samples treated at 100 °C, and a few octahedral grains along the defect lines attributed to the polishing process of the substrate on the sample treated at higher temperatures (Fig. 8). These lines were also detected by AFM on the as-received single crystal surfaces. The surface free of

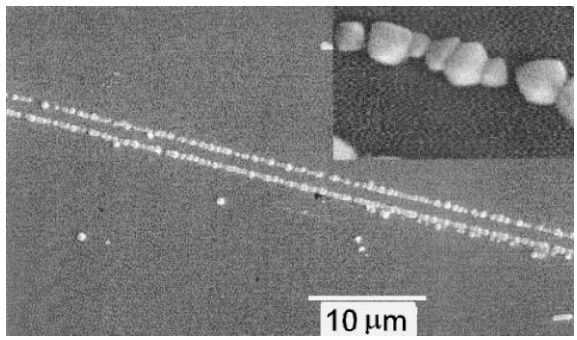

Fig. 8. SEM micrograph of a $TiO_2(1\,1\,0)$ sample treated 4 h at 150 °C.

grains was as smooth as the single crystal without any treatment.

3.2.3. Composition

RBS spectra displayed a small barium signal in the whole set of sample. Its height was close to the limit detection of this technique. Consequently, in order to have a better resolution XPS was used.

XPS measurements displayed titanium, barium, oxygen, and carbon signals in the surfaces of all samples. The Ba 3d peak was weak and easily removed after a single erosion of ~5 mC/cm^2 Ar^+ ions (Fig. 9).

A rough quantitative estimate is provided by the peak-to-peak amplitude of the Ba 3d5/2 and Ti 2p3/2 photoelectron signals, which were compared with the spectrum of a $BaTiO_3$ single crystal (not shown), used as a stoichiometric reference. Before sputtering, the ratio of Ba:Ti is around 1:10 and reduces to Ba:Ti = 1:100 after sputtering. This can be interpreted either as a homogeneous compound poor in barium or as stoichiometric $BaTiO_3$ islands covering around 1% of the surface. Only the latter is consistent with the SEM data. The higher barium content before sputtering is attributed to residuals left on the surface when the sample is removed from the solution.

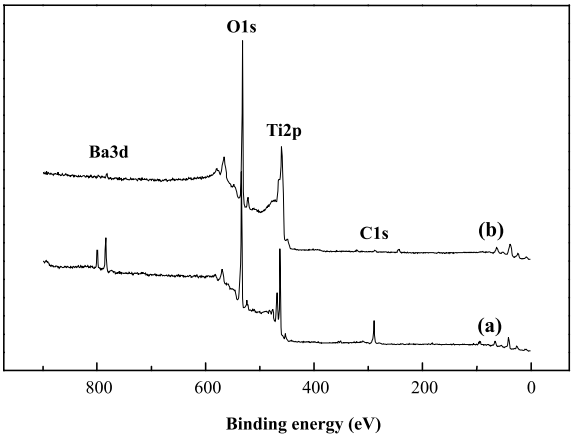

Fig. 9. XPS spectra of the TiO_2(1 1 0) substrates treated in a hydrothermal bath at 200 °C. The recordings show the (a) as-deposited surface and (b) the one after a single 5 mC/cm^2 Ar^+ dose erosion.

4. Discussion

Different TiO_2 orientations treated under the same conditions lead to the same crystal growth habit. However, the growth rates are completely different between the (0 0 1) orientation, where island (150 °C) or film growth occurs (200 °C), and the (1 1 0) orientation, where at the highest temperatures only a few grains are observed. Since for the 1 1 0 oriented single crystals, grown grains are located along the defect-rich lines caused by the polishing process, where many different orientations are exposed, it follows that there is no growth at all at the defect-free (1 1 0) face. These results are consistent with a growth model based on a dissolution process. The (1 1 0) face of TiO_2 is the most stable face of this oxide, according to its thermodynamic properties [20]. At the same time, the (0 0 1) surface is the less stable face among the low-indexed faces [21]. Therefore it should be easier to dissolve material from the (0 0 1) surface than from the (1 1 0) one. Extended defects on TiO_2(1 1 0), such as polish lines, would leave the less stable surfaces partially exposed, which would be easier to dissolve. It is worth to note that this very localized deposition may be used to control selective $BaTiO_3$ growth on appropriate pattern TiO_2 surfaces.

Small amounts of strontium strongly affect the growth habit: the strontium-rich reagent leads to hemispherical polycrystalline grains, whereas the high purity reagent leads to single crystal, octahedral shaped, (1 1 1) terminated crystallites. The crystal habit of grains grown from solution is affected by the temperature and the impurities, and is determined by the relative growth rates of its faces [22,23]. The slower the growth rate in the direction perpendicular to a certain face, the larger that face appears, forming finally the crystal shape. Impurities reduce this growth velocity and, in certain cases, block completely the advance of one face. During crystal growth, the impurities might be adsorbed preferentially on certain crystal faces, and the affected faces will appear larger than the non-affected ones, changing the crystal habit. We suggest that the different crystal habits observed at different strontium impurity levels in the solution are caused by strontium blocking of the

preferred growth directions at higher strontium content.

One of the interesting results reported in this paper is the coexistence of the cubic and tetragonal $BaTiO_3$ phases on the same film, which is a fact observed only on samples prepared with the strontium-rich reagent. Presently we have no explanation regarding the effect of the small amount of strontium. However, it has been reported that both phases of $BaTiO_3$ can coexist in ultrafine powders grown by a sol–crystal method, and that the relative amount of the cubic phase increases with decreasing particle size [24]. This is consistent with our identification of the cubic phase in the fine-grained region of Fig. 2 and with the tetragonal one in the large grains of the same figure. Notice that these large grains are not single crystals, as indicated by the different contrast regions in each grain. The coexistence of both phases in the same single-crystalline grain has been reported by Takeuchi et al. for samples prepared by conventional solid state reaction [25]. A direct comparison to our results is not possible, since, besides the different preparation conditions, we do not report on single-crystalline grains. Finally, it is known that chlorine ions favor the growth of the tetragonal phase under hydrothermal conditions [26], but the reported chlorine concentration in those experiment is around 0.25 M, much higher than the highest chlorine content of any of our reactants, which is less than 0.003 wt.% in the high purity and less than 0.005 wt.% in the strontium-rich one.

Based on the TEM results, the diffractogram of the sample treated at 200 °C with the Sr-rich reagent has to be reinterpreted. This recording is formed by a combination of cubic and tetragonal phases, clearly distinguishable by the two (1 1 1) reflexes (See Fig. 1b, $2\Theta \sim 39°$). Attributing the signals with the highest intensities to the cubic phase, the calculated lattice parameter is 0.3996(1) nm. The tetragonal phase shares these reflections with the cubic one, but its (1 1 1) signal is that with the lowest intensity ($2\Theta = 38.74°$). Thus, the calculated lattice parameters for the tetragonal phase are 0.3994(4) and 0.4010(6) nm. A quantitative estimate of relative concentration of the cubic and tetragonal phases is provided by the comparison of the two (1 1 1) peak heights (inset Fig. 1b), leading to a cubic:tetragonal ratio of 2.7:1. The estimate was also performed from the TEM cross-sectionals views (Fig. 2). The relative thickness of the fine grained and large grained regions is different among different micrographs, with an average of cubic:tetragonal of 3.4:1, which is an acceptable agreement for such a crude estimate.

The RBS measurements of samples prepared with the high-purity reagent indicate no measurable strontium incorporation. On the other hand, the strontium content of the samples grown with the strontium-rich reagent was higher than the solution content, which is consistent with other reports [3,8]. This strontium content value is in agreement with that estimated independently from the lattice parameter. In fact, by means of the relation found by Kajiyoshi et al. (Fig. 4 in Ref. [8]) for $(Ba,Sr)TiO_3$ thin film solid solutions, the lattice parameter of 0.399 nm corresponds to a strontium content of ~10 at.%. Therefore, one can consider that the lattice parameters found in the present paper are an extension of the work done in Ref. [8] for the extreme case of very low strontium concentrations.

5. Conclusions

The use of two grades of $Ba(OH)_2$ with different amounts of strontium ions demonstrated that this impurity strongly affects the morphology of the hydrothermal $BaTiO_3$ film grown on TiO_2(0 0 1) substrates. The high purity hydroxide allowed the formation of deposits with a pronounced crystal habit with octahedral grains. The faces of these octahedrons correspond to the {1 1 1} family of planes. A less pure reagent, with higher strontium content, lead to layered films, a fine sized layer of cubic $BaTiO_3$ in contact with the TiO_2 substrate, and large tetragonal grains on top, which covers approximately 25% of the film.

Different orientations of the TiO_2 single crystal exposed to the aqueous $Ba(OH)_2$ solution displayed different behaviors. $BaTiO_3$ grew on the (0 0 1) surface at temperatures as low as 100 °C, while the TiO_2(1 1 0) surface did not produce $BaTiO_3$ grains even at 200 °C. This is consistent with a growth model involving a dissolution process,

since the (1 1 0) surface is the most stable face of TiO_2.

Acknowledgements

This work was supported by grants Fondecyt 2950026, 1970310, and FONDAP 11980002 and Fundación Andes C-12510 and C-10810/2. We want to thank Dr. J. Santiago-Avilés for the help provided. SEM micrographs (Fig. 5a and f), WDS, and EDX analysis were possible thanks to the use of MRSEC shared experimental facilities of the University of Pennsylvania (equipment supported by the NSF under Award DMR96-35598). Sample preparation was performed at the Chilean Nuclear Energy Commission. The high purity $Ba(OH)_2$ was provided by courtesy of Solvay-Sabed, Inc. We also acknowledge the photographic work performed by Mr. José Morillas (Pontificia Universidad Católica de Chile) and Mr. Rafael Ropero (Instituto de Ciencia de Materiales de Madrid, CSIC, Spain).

References

[1] M. Yoshimura, S. Yoo, M. Hayashi, N. Ishizawa, Jpn. J. Appl. Phys. 28 (1989) L2007.
[2] N. Hayashi, N. Ishizawa, S. Yoo, M. Yoshimura, J. Ceram. Soc. Jpn. 98 (1990) 930.
[3] M. Pilleux, V.M. Fuenzalida, J. Appl. Phys. 74 (1993) 4664.
[4] V.M. Fuenzalida, J.G. Lisoni, N.I. Morimoto, J.C. Acquadro, Appl. Surf. Sci. 108 (1997) 385.
[5] S. Venigalla, P. Bendale, J.H. Adair, J. Electrochem. Soc. 142 (1995) 2101.
[6] K. Kajiyoshi, N. Ishizawa, M. Yoshimura, J. Am. Ceram. Soc. 74 (1991) 369.
[7] E.B. Slamovich, I.A. Aksay, J. Am. Ceram. Soc. 79 (1996) 239.
[8] K. Kajiyoshi, M. Yoshimura, Y. Hamaji, K. Tomono, T. Kasanami, J. Mater. Res. 11 (1996) 169.
[9] J.O. Eckert Jr., C.C. Hung-Houston, B.L. Gersten, M. Lencka, R. Riman, J. Am. Ceram. Soc. 79 (1996) 2929.
[10] W. Hertl, J. Am. Ceram. Soc. 71 (1988) 879.
[11] N. Ishizawa, M. Hayashi, H. Banno, S. Mizunuma, H. Yamaguchi, S.E. Yoo, M. Yoshimura, Report of the Research Laboratory of Engineering Materials, Tokyo Institute of Technology, vol. 16, 1991, p. 9.
[12] P. Bendale, S. Venigalla, J.R. Ambrose, E.D. Verink Jr., J.H. Adair, J. Am. Ceram. Soc. 76 (1993) 2619.
[13] T. Vargas, H. Díaz, C.I. Silva, V.M. Fuenzalida, J. Am. Ceram. Soc. 80 (1997) 213.
[14] I.S. Escobar, C.I. Silva, T. Vargas, V.M. Fuenzalida, J. Am. Ceram. Soc. 83 (2000) 2673.
[15] Z. Wu, M. Yoshimura, Solid State Ionics 122 (1999) 161.
[16] W. Zhu, S.A. Akbar, R. Asiaie, P.K. Dutta, J. Electroceram. 2 (1998) 21.
[17] W.-P. Xu, L. Zheng, C. Lin, M. Okuyama, Integrated Ferroelectrics 12 (1996) 233.
[18] M.E. Pilleux, C.R. Grahmann, V.M. Fuenzalida, R.E. Avila, Appl. Surf. Sci. 65/66 (1993) 283.
[19] E.H. de Geleen, Ph. D. Thesis no. 2193, Faculty of Science, University of Gèneve, France, 1986, pp. 95–109 (in English).
[20] V.E. Henrich, R.L. Kurtz, Phys. Rev. B 23 (1981) 6280.
[21] V.E. Henrich, P.A. Cox, The Surface Science of Metal Oxides, Cambridge University Press, London, 1994, pp. 42–49.
[22] K. Sangwal, Prog. Cryst. Growth Charact. 32 (1996) 3.
[23] W. van Enckevort, A. van der Berg, K. Kreuwel, A. Derksen, M. Couto, J. Cryst. Growth 166 (1996) 156.
[24] T. Takeuchi, M. Tabuchi, K. Ado, K. Honjo, O. Nakamura, H. Kageyama, Y. Sunama, N. Ohtori, M. Nagasawa, J. Mater. Sci. 32 (1997) 4053.
[25] T. Takeuchi, K. Ado, T. Asai, H. Kageyama, Y. Saito, C. Masquelier, O. Nakamura, J. Am. Ceram. Soc. 77 (1994) 1665.
[26] P.K. Dutta, J.R. Gregg, Chem. Mater. 4 (1992) 843.